

Intramolecular Delayed Fluorescence as a Tool for Imaging Science: Synthesis and Photophysical Properties of a First-Generation Emitter

Andrew C. Benniston, Anthony Harriman,* Irantzu Llarena, and Craig A. Sams

Molecular Photonics Laboratory, Bedson Building, School of Natural Sciences, Newcastle University, Newcastle upon Tyne NE1 7RU, United Kingdom

Received October 23, 2006. Revised Manuscript Received February 10, 2007

The synthesis of a molecular dyad comprising two pyrene-based terminals covalently linked via a Hantzsch 1,4-dihydropyridine is described. The dyad is sufficiently flexible to allow the end groups to approach each other in fluid solution, as is evident from the appearance of excimer fluorescence. Transient absorption spectroscopy indicates that both intra- and intermolecular triplet–triplet annihilation (TTA) takes place at modest laser intensities and leads to delayed fluorescence. The spectral distribution of the delayed fluorescence signal matches that of the excimer. The kinetics of TTA and the overall yield of delayed fluorescence are considered in terms of the molecule adopting disparate conformations that interconvert slowly. Consideration is also given to the possible application of such delayed fluorescence in imaging technology.

Introduction

Comprehension of how molecular entities behave in their normal operating environment is indispensable information required in many areas of science, including biology,¹ chemistry,² and medicine.³ Probing a species and gaining insightful information can be a major challenge, however, particularly in what sometimes can be difficult surroundings. Attention has turned recently to the use of chemical sensors to report on an assortment of analytes (e.g., cations,⁴ anions,⁵ proteins,⁶ DNA⁷) in various media. For such systems to be of genuine benefit it is essential that there is a clear on/off

signal, or sharp contrast, that can be readily relayed to the observer.⁸ A further crucial requisite for such sensors concerns their specificity for the phenomenon under investigation. Detection and, hence, feed-back methods have now been developed that respond to, for example, redox changes (glucose sensing),⁹ particle emission (positron emission tomography),¹⁰ radiowave signals (MRI),¹¹ and radiation emission (gamma ray spectroscopy).¹² Many other systems rely on the emission of visible light (fluorescence or phosphorescence) from molecular entities as a non-intrusive signaling method.¹³ An important advantage of emission spectroscopy relates to the realization that detection can be carried out by either steady-state¹⁴ or time-resolved modes.¹⁵

A major problem associated with luminescent chemical sensors concerns resolving the “real” signal from background

* To whom correspondence should be addressed. E-mail: anthony.harriman@ncl.ac.uk. Telephone and fax: (44) (0)191222 8660.

- (1) (a) Mendintz, I. L.; Uyeda, H. T.; Goldman, E. R.; Mattoussi, H. *Nat. Mater.* **2005**, *4*, 435. (b) Yotter, R. A.; Wilson, D. M. *IEEE Sens. J.* **2004**, *4*, 412. (c) Myra, S. *Biosens. Bioelectron.* **2004**, *19*, 1345.
- (2) (a) Parker, D. *Chem. Soc. Rev.* **2004**, *33*, 156. (b) de Silva, A. P.; McCaughan, B.; McKinney, B. O. F.; Querol, M. *Dalton Trans.* **2003**, 1902.
- (3) (a) O’Neil, R. D.; Lowry, J. P.; Mas, M. *Crit. Rev. Neurobiol.* **1998**, *12*, 69. (b) Thompson, R. B. *Curr. Opin. Chem. Biol.* **2005**, *9*, 526.
- (4) (a) de Silva, A. P.; Gunaratne, H. Q. N.; Gunnlaugsson, T.; Huxley, A. J. M.; McCoy, C. P.; Rademacher, J. D.; Rice, T. E. *Chem. Rev.* **1997**, *97*, 1515. (b) Fabrizzi, L.; Poggi, A. *Chem. Soc. Rev.* **1995**, *24*, 197.
- (5) (a) Davis, F.; Collyer, S. D.; Higson, S. P. J. *Topics Curr. Chem.* **2005**, *255*, 97. (b) Suksai, C.; Tuntulani, T. *Chem. Soc. Rev.* **2003**, *32*, 192. (c) Fabbri, L.; Licchelli, M.; Taglietti, A. *Dalton Trans.* **2003**, 3471. (d) Beer, P.; Cadman, J. *Coord. Chem. Rev.* **2000**, *205*, 131.
- (6) (a) Bilewiski, U. *Anal. Chim. Acta* **2006**, *568*, 232. (b) Wang, Z.; Wilkop, T.; Cheng, Q. *Langmuir* **2005**, *21*, 10292. (c) Ikebukuro, K.; Kiyohara, C.; Sode, K. *Biosens. Bioelectron.* **2005**, *20*, 2168. (d) Zadnarm, R.; Schrader, T. *J. Am. Chem. Soc.* **2005**, *127*, 904. (e) Santos, M.; Roy, B. C.; Goicoechea, H.; Campiglia, A. D.; Mallik, S. *J. Am. Chem. Soc.* **2004**, *126*, 10738. (f) Lasseter, T. M.; Clare, B. H.; Abbott, N. L.; Hamers, R. J. *J. Am. Chem. Soc.* **2004**, *126*, 10220.
- (7) (a) Narita, A.; Ogawa, K.; Sando, S.; Aoyama, Y. *Angew. Chem., Int. Ed.* **2006**, *45*, 2879. (b) Charych, D. H.; Nagy, J. O.; Spevak, W.; Bednarski, P. *Science* **1993**, *261*, 585. (c) Albrecht, C.; Blank, K.; Lalic-Multhaler, M.; Hirler, S.; Mai, T.; Gilbert, I.; Schiffman, S.; Bayer, T.; Clausen-Schaumann, H.; Gaub, H. *Science* **2003**, *301*, 367.
- (8) Marriott, G.; Clegg, R. M.; Arndt-Jovin, D. J.; Jovin, T. M. *Biophys. J.* **1991**, *60*, 1374.
- (9) Bernhardt, P. V. *Aust. J. Chem.* **2000**, *59*, 233.
- (10) Anderson, C. J.; Welch, M. J. *Chem. Rev.* **1999**, *99*, 2219.
- (11) (a) Parker, D.; Dickins, R. S.; Puschmann, H.; Crossland, C.; Howard, J. A. K. *Chem. Rev.* **2002**, *102*, 1977. (b) Caravan, P.; Ellison, J. J.; McMurtry, T. J.; Lauffer, R. B. *Chem. Rev.* **1999**, *99*, 2293.
- (12) Tang, J.; Top, S.; Vessières, A.; Sellier, N.; Vaissermann, J.; Jaouen, G. *Appl. Organomet. Chem.* **1997**, *11*, 771.
- (13) (a) Xu, S.; Lui, B.; He, T. *Prog. Chem.* **2006**, *18*, 687. (b) Martínez-Máñez, R.; Sancenón, F. *J. Fluoresc. Chem.* **2005**, *15*, 267. (c) Gunnlaugsson, T.; Ali, H. D. P.; Glynn, M.; Kruger, P. E.; Hussey, G. M.; Pfeffer, F. M.; dos Santos, C. M. G.; Tierney, J. *J. Fluoresc. Chem.* **2005**, *15*, 287. (d) Pickup, J. C.; Hussain, F.; Evans, N. D.; Rolinski, O. J.; Birch, D. J. S. *Biosens. Bioelectron.* **2005**, *20*, 2555. (e) Pina, F.; Bernardo, M. A.; García-España, E. *Eur. J. Inorg. Chem.* **2000**, 2143. (f) de Silva, A. P.; Gunnlaugsson, T.; Rice, T. E. *Analyst* **1996**, *121*, 1759.
- (14) (a) Li, Y. Q.; Bricks, J. L.; Resch-Genger, U.; Spieles, M.; Rettig, W. *J. Phys. Chem. A* **2006**, *110*, 10972. (b) Pina, J.; Seixas, de Melo, J.; Pina, F.; Lodeiro, C.; Lima, J. C.; Parola, A. *J. Inorg. Chem.* **2005**, *44*, 7449. (c) Cody, J.; Farhani, C. *J. Tetrahedron* **2004**, *60*, 11099. (d) Geddes, C. D.; Douglas, P.; Moore, C. P.; Wear, T. J.; Egerton, P. L. *Dyes Pigm.* **1999**, *43*, 59.
- (15) (a) Pandya, S.; Lu, Y.; Parker, D. *Dalton Trans.* **2006**, 2757. (b) Lin, Z.; Wu, M.; Wolfbeis, O. S. *Chirality* **2005**, *17*, 464. (c) Schaferling, M.; Wu, M.; Wolfbeis, O. S. *J. Fluoresc.* **2004**, *14*, 561.

fluorescence and/or scattering.¹⁶ This limitation arises from a number of factors, including the difficulty in selectively exciting the probe molecule, overlap of multiple luminescence signals, and fast time scale (picoseconds to nanoseconds) associated with fluorescence decay. Time-gated techniques¹⁵ have alleviated, at least to some extent, the problem but necessitate the use of stable molecules that emit strongly on relatively slow time scales (i.e., milliseconds). Luminescent lanthanide complexes have been identified as prime candidates for such sensors,¹⁷ essentially because they possess inherently long decay times and emission profiles that occur in the visible to near-infrared spectral region. Because molar absorption coefficients associated with lanthanide f–f transitions are relatively weak, sensitization by aromatic moieties attached to the complex is needed.¹⁸ Other approaches to this end have involved searching for ways to prolong the phosphorescence decay times of transition metal complexes.¹⁹

In an attempt to improve existing sensor technology based on fluorescent molecules, we have turned our attention to the use of delayed fluorescence (DF).²⁰ The process of DF can arise by way of thermal repopulation of the fluorescent state if the singlet–triplet (S–T) energy gap is relatively small. A more versatile way to generate DF, however, is via triplet–triplet annihilation (TTA) in fluid media.²¹ For this process, the S–T energy gap can be large provided it is less than twice the triplet energy. Moreover, the process of TTA corresponds to triplet-energy transfer and requires overlap of the respective orbitals on the reacting molecules. This occurs through diffusive contact in fluid solution but can also involve intramolecular TTA if a chromophore is equipped with two photoactive units. The process of TTA forms a ground-state molecule and a molecule promoted to the first excited singlet state, although other excited-state species are often produced. The key feature of TTA is that the fluorescence decay time matches that of the precursor triplet state. Instead of the normal fluorescence decay time of a few nanoseconds, DF can survive for some tens of microseconds. In certain cases, TTA can lead to excimer formation, and this has additional benefits for fluorescence sensing since it leads to an enhanced Stokes' shift.²²

While bimolecular TTA has been studied over many decades,²³ much less is known about the corresponding

intramolecular process. The most popular chromophores are anthracene and pyrene, and considerable attention has been given to understanding the mechanism of bimolecular TTA with such polycycles.²⁴ Here, we consider the intramolecular case and describe a prototypic molecular dyad comprising two pyrene-based fluorophores linked via a Hantzsch 1,4-dihydropyridine (DHP) unit. The system is flexible, and the two pyrene terminals can approach each other so as to form an intramolecular excimer, as documented in numerous related dyads. Our motivation for studying this dyad is to critically examine if sufficient DF can be generated to propose using such dyads as advanced fluorescent sensors. This requires measurement of the decay times for prompt and delayed fluorescence, consideration of the role of the excimer, and knowledge of the triplet state.

Experimental Section

All chemicals were purchased from commercial sources and were used as received. The starting material pyrene-1-carbonyl chloride was made by a literature method.²⁵ Solvents for synthesis were dried by standard literature methods before being distilled and stored under nitrogen over 4 Å molecular sieves.²⁶ ¹H and ¹³C NMR spectra were recorded with a Bruker AVANCE 300 MHz spectrometer. Routine mass spectra and elemental analyses were obtained using in-house facilities. Cyclic voltammetry studies were performed using a fully automated HCH Instruments electrochemical analyzer, with a three-electrode setup comprising a glassy carbon working electrode, a Pt wire counter electrode, and an Ag wire reference. All experiments were performed in dry CH₂Cl₂ containing *N*-tetrabutylammonium tetrafluoroborate (0.2 M) as background electrolyte. Ferrocene was used as the redox standard, and potentials were rescaled to SCE using the conversion factor that $E_{1/2}(\text{Fc}/\text{Fc}^+) = +0.45$ V versus SCE. The concentration of solute was approximately 2.4 mM.

Absorption spectra were recorded with a Hitachi U3310 spectrometer while steady-state fluorescence spectra were recorded with a Yvon-Jobin Fluorolog tau-3 spectrophotometer. All fluorescence measurements were made using optically dilute solutions and were corrected for spectral imperfections of the instrument by reference to a standard lamp. Quantum yield measurements were made relative to 9,10-diphenylanthracene.²⁷ Time-resolved fluorescence measurements were made by time-correlated, single-photon counting with excitation at 340 nm. The excitation source was a fast laser diode (full width at half-maximum, fwhm = 300 ps), and detection was made with a microchannel plate photocell. The instrumental response function was deconvoluted from the fluorescence signal using a Ludox scattering curve recorded at the excitation wavelength and normalized by computer iteration. The goodness-of-fit was assessed by the usual criteria,²⁸ and the kinetic parameters were derived on the basis of a compartmentalized analysis²⁹ carried out over 40 separate detection wavelengths. The

(16) Prodi, L. *New J. Chem.* **2005**, 29, 20.

(17) (a) Parker, D. *Chem. Soc. Rev.* **2004**, 33, 120. (b) Leonard, J. P.; Gunnlaugsson, T. *J. Fluoresc.* **2005**, 15, 585. (c) Hanaoka, K.; Kukuchi, K.; Kojima, H.; Urano, Y.; Nagano, T. *J. Am. Chem. Soc.* **2004**, 126, 12470. (d) Gunnlaugsson, T.; Leonard, J. P.; Sénéchal, K.; Harte, A. J. *Chem. Commun.* **2004**, 782. (e) Gunnlaugsson, T.; Leonard, J. P.; Sénéchal, K.; Harte, A. J. *J. Am. Chem. Soc.* **2003**, 125, 12062.

(18) (a) Parker, D.; Williams, J. A. G. *J. Chem. Soc., Perkin Trans 2*, **1995**, 1305. (b) Parker, D.; Williams, J. A. G. *J. Chem. Soc. Dalton Trans.* **1996**, 3613.

(19) Hissler, M.; Harriman, A.; Khatyr, A.; Ziessel, R. *Chem.—Eur. J.* **1999**, 5, 3366.

(20) Fister, J. C., III; Rank, D.; Harris, J. M. *Anal. Chem.* **1995**, 67, 5269.

(21) Angulo, G.; Grampp, G.; Neufeld, A. A.; Burshtein, A. I. *J. Phys. Chem. A* **2003**, 107, 6913.

(22) Ohkita, H.; Ito, S.; Yamamoto, M.; Tohda, Y.; Tani, K. *J. Phys. Chem. A* **2002**, 106, 2140.

(23) (a) Stevens, B.; Hutton, E. *Nature* **1960**, 186, 1045. (b) Parker, C. A.; Hatchard, C. G. *Proc. Chem. Soc.* **1962**, 147. (c) Parker, C. A.; Hatchard, C. G. *Trans. Faraday Soc.* **1963**, 59, 284. (d) Parker, C. A. *Adv. Photochem.* **1964**, 2, 305.

(24) (a) Linschitz, H.; Pekkarinen, L. *J. Am. Chem. Soc.* **1960**, 82, 2411. (b) Jackson, G.; Livingston, R. *J. Chem. Phys.* **1961**, 35, 2182. (c) Livingston, R.; Ware, W. R. *J. Chem. Phys.* **1963**, 39, 2593. (d) Porter, G.; Wright, M. R. *Discuss. Faraday Soc.* **1959**, 27, 94. (e) Watkins, A. R. *Z. Phys. Chem. (Frankfurt am Main)* **1975**, 96, 125. (f) Grellmann, J. H.; Scholz, H. G. *Chem. Phys. Lett.* **1979**, 62, 64.

(25) D'Souza, L. J.; Maitra, U. *J. Org. Chem.* **1996**, 61, 9494.

(26) Perrin, D. D.; Armarego, W. L. F. *Purification of Laboratory Chemicals*, 3rd ed.; Pergamon Press, Ltd.: Oxford, 1988.

(27) Morris, J. V.; Mahaney, M. A.; Huber, J. R. *J. Phys. Chem.* **1976**, 80, 969.

(28) O'Connor, D. V.; Phillips, D. *Time-Correlated Single Photon Counting*; Academic Press: New York, 1984.

temporal resolution of this setup was approximately 400 ps. Solutions were optically dilute and deoxygenated with a stream of dried N₂. All measurements were made over a series of time bases.

Laser flash photolysis studies were made with an Applied Photophysics Ltd. LKS.60 setup using a frequency-tripled Nd:YAG (fwhm = 4 ns) laser pumped optical parametric oscillator. Solutions were purged with dried N₂ and adjusted to possess an absorbance of approximately 0.3 at the excitation wavelength. Transient absorption spectra were recorded point-by-point using a pulsed Xe arc lamp as the monitoring beam. DF was recorded without the monitoring beam. The signal was passed through a high-radiance monochromator and directed to a fast response photomultiplier tube and then to a transient recorder for averaging and storage. Laser intensities were adjusted with crossed polarizers and measured with a Gentec power meter, using a beam splitter to reflect 5% of the excitation pulse. Corrections were made for minor variations in pulse energies, and at least 100 individual laser shots were averaged for each measurement. The relative quantum yield for DF was measured by integration of the kinetic trace at a given laser power. The initial concentration of chromophore was varied over a wide range. The optical setup was calibrated by reference to phosphorescence from ruthenium(II) tris(2,2'-bipyridine)³⁰ in deoxygenated acetonitrile, and a wavelength correction curve was generated using a standard lamp.

Preparation of 3-Hydroxypropyl Pyrene-1-carboxylate (1).

To a 50 mL round-bottom flask under nitrogen were added ethylene glycol (0.16 mL, 3 mmol), freshly distilled pyridine (0.01 mL, 0.11 mmol), and CH₂Cl₂ (5 mL). Pyrene-1-carbonyl chloride (250 mg, 1 mmol) dissolved in CH₂Cl₂ (20 mL) was added dropwise to the solution at room temperature, and the mixture was allowed to stir for a further 24 h. The sample was extracted with ethyl acetate and washed with brine. The combined organic layers were dried over MgSO₄, filtered, and concentrated. Purification of the crude material by column chromatography using silica gel and CH₂Cl₂ as the eluant afforded a yellow solid which when recrystallized from CH₂Cl₂/petroleum ether afforded a white solid. Yield: 230 mg, 0.79 mmol, 68%. ¹H NMR (300 MHz, CDCl₃): δ = 1.50 (s, 4H), 7.99–8.24 (m, 7H), 8.73 (d, 1H, J = 8.61 Hz), 9.29 (d, 1H, J = 9.44 Hz). ¹³C NMR (300 MHz, CDCl₃): δ = 61.93, 67.18, 123.61, 124.34, 124.54, 125.15, 126.52, 126.60, 126.61, 127.39, 128.70, 129.81, 129.96, 130.75, 131.38, 131.58, 134.80, 168.57 (note: one carbon is accidentally equivalent). EI-MS m/z calcd for C₁₉H₁₄O₃, 290.32; found, 290. Anal. Calcd for C₁₉H₁₄O₃·H₂O: C, 74.01; H, 5.23. Found: C, 74.81; H, 4.19. Mp = 88–90 °C.

Preparation of 2-(3-Oxobutanoyloxy)ethyl Pyrene-1-carboxylate (2). To a three-necked flask under nitrogen was added 3-hydroxypropyl pyrene-1-carboxylate (150 mg, 0.51 mmol) dissolved in distilled benzene (10 mL). Freshly distilled pyridine (0.5 mL) was added, and the mixture was cooled in an ice bath. To the solution was added dropwise diketene (0.04 mL, 0.44 mmol). The reaction was refluxed for 1 h, during which the mixture changed color from light yellow to orange. After cooling to room temperature, the product was extracted with CH₂Cl₂ and washed with water. The combined organics were dried over MgSO₄, filtered, and evaporated. The crude orange product was purified by column chromatography on silica gel, using CH₂Cl₂/Et₂O (1:1) as the eluant to afford a yellow oil. Yield: 150 mg, 0.4 mmol, 80%. ¹H NMR (300 MHz, CDCl₃): δ = 9.20 (d, 1H, J = 9.5 Hz), 8.58 (d, 1H, J = 8.1 Hz), 8.20 (m, 5H), 8.03 (dd, 2H, J = 8.3 Hz, J' = 4.1 Hz), 4.60 (m, 4H), 3.47 (s, 2H), 2.20 (s, 3H). ¹³C (300 MHz, CDCl₃):

δ = 173.78, 173.75, 134.72, 131.22, 129.83, 129.65, 128.57, 127.26, 127.21, 126.40, 126.33, 125.03, 124.98, 124.92, 124.18, 63.27, 62.62, 52.19, 48.89 (note: 19 of the 23 signals were observed). EI-MS m/z calcd for C₂₃H₁₈O₅, 374.4; found, 374.

Preparation of PDHP. 2-(3-Oxobutanoyloxy)ethyl pyrene-1-carboxylate, **2**, (150 mg, 0.4 mmol) was placed in a 25 mL round-bottom flask containing NH₄OAc (16 mg, 0.2 mmol) and benzaldehyde (0.02 mL, 0.2 mmol). The flask was placed under a nitrogen atmosphere, and the mixture was heated to 120 °C for 30 min. After allowing the reaction mixture to cool to room temperature, the thick brown oil was purified by column chromatography on silica gel using CH₂Cl₂ as the eluant. The yellow oil collected was recrystallized by slow vapor diffusion of petroleum ether into a CH₂Cl₂ solution of the material. Yield: 20 mg, 0.024 mmol, 6%. ¹H NMR (DMSO-*d*₆, 300 MHz): δ = 8.99 (d, 1H, J = 9.4 Hz), 8.92 (s, 1H), 8.25 (m, 18H), 7.18 (d, 2H, J = 7.2 Hz), 6.90 (t, 2H, J = 7.3 Hz), 6.81 (t, 2H, J = 7.2 Hz), 5.75 (s, 1H), 5.03 (s, 1H), 4.5 (m, 4H), 2.25 (s, 6H). ¹³C (300 MHz, DMSO-*d*₆): δ = 167.21, 167.14, 148.25, 146.35, 134.14, 130.89, 130.42, 130.09, 129.95, 129.63, 128.45, 128.05, 127.50, 127.40, 126.97, 126.88, 126.56, 126.02, 124.56, 124.46, 124.21, 123.63, 120.19, 63.50, 61.61, 55.14, 30.93, 18.57. EI-MS m/z calcd for C₅₃H₃₉N₁O₈, 817.9; found, 817. Anal. Calcd for C₅₃H₃₉N₁O₈·5H₂O: C, 70.11; H, 5.44, N, 1.54. Found: C, 70.15; H, 4.46; N, 1.17.

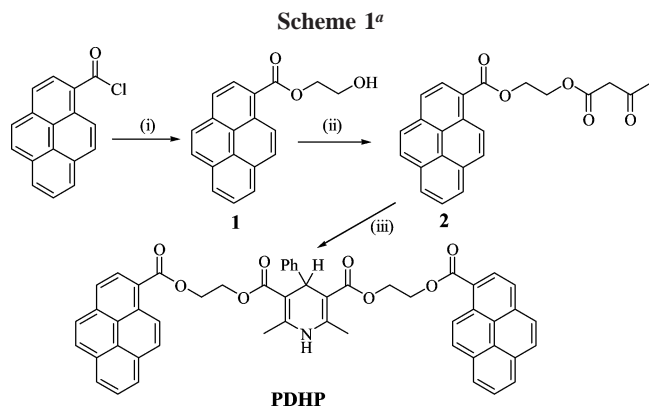
Results and Discussion

Design, Synthesis and Electrochemistry of the Target Compound. An inordinately wide variety of systems are known that allow the precise positioning of two pyrene terminals separated by spacers of disparate flexibility and composition. These include alkyl chains,³¹ acetylene units,³² disulfide linkers,³³ crown ethers,³⁴ azamacrocycles,³⁵ chelates,³⁶ calixarenes,³⁷ and natural products,³⁸ to name but a few. Close examination of these spacers reveals that they can be characterized into two categories: (i) flexible chains of varying length or (ii) centrally functionalized with recognition sites for host–guest chemistry. This latter theme is a popular approach for building fluorescence sensors that operate by way of the binding process interrupting excimer formation.³⁹ In designing a conjugate that would display DF,

(29) Verbeeck, A.; De Schryver, F. C. *Langmuir* **1986**, *3*, 494.

(30) (a) Demas, J. N.; Crosby, G. A. *J. Am. Chem. Soc.* **1971**, *93*, 2741. (b) El-ghayoury, A.; Harriman, A.; Khatyr, A.; Ziessel, R. *J. Phys. Chem. A* **2000**, *104*, 1512.

(31) (a) Snare, M. J.; Thistlewaite, P. J.; Ghiggino, K. P. *J. Am. Chem. Soc.* **1983**, *105*, 3328. (b) Tanaya, T.; Goshiki, K.; Yamamoto, M.; Nishijima, Y. *J. Am. Chem. Soc.* **1982**, *104*, 3580. (c) Anderson, V. C.; Weiss, R. G. *J. Am. Chem. Soc.* **1984**, *106*, 6628. (32) Benniston, A. C.; Harriman, A.; Lawrie, D. J.; Rostron, S. A. *Eur. J. Org. Chem.* **2004**, *10*, 2272. (33) Beckwith, A. L. J.; Low, B. S. *J. Chem. Soc.* **1964**, 2571. (34) (a) Kubo, K.; Sukurai, T. *Chem. Lett.* **1996**, *11*, 959. (b) Collins, G. E.; Choi, L. S. *Chem. Commun.* **1997**, 1135. (c) Kubo, K.; Kato, N.; Sakurai, T. *Bull. Chem. Soc. Jpn.* **1997**, *70*, 3041. (35) Moon, S. Y.; Youn, N. J.; Park, S. M.; Chang, S. K. *J. Org. Chem.* **2005**, *70*, 2394. (36) (a) Ziessel, R.; Stroth, C. *Tetrahedron Lett.* **2004**, *45*, 4051. (b) Maubert, B.; McClenaghan, N. D.; Indelli, M. T.; Campagna, S. *J. Phys. Chem. A* **2003**, *107*, 447. (37) (a) van der Veen, N. J.; Flink, S.; Deij, M. A.; Egberink, R. J. M.; van Veggel, F. C. J. M.; Reinhoudt, D. N. *J. Am. Chem. Soc.* **2000**, *122*, 6112. (b) Lee, J. Y.; Kim, S. K.; Jung, J. H.; Kim, J. S. *J. Org. Chem.* **2005**, *70*, 1463. (c) Kim, S. K.; Lee, S. H.; Lee, J. Y.; Bartsch, R. A.; Kim, J. S. *J. Am. Chem. Soc.* **2004**, *126*, 16499. (38) Xu, M.; Nishino, N.; Mihara, H.; Fujimoto, T.; Izumiya, N. *Chem. Lett.* **1992**, *2*, 191. (39) (a) Schazmann, B.; Alhashimy, N.; Diamond, D. *J. Am. Chem. Soc.* **2006**, *128*, 8607. (b) Suzuki, Y.; Morozumi, T.; Nakamura, H.; Shimomura, M.; Hayashita, T.; Bartsch, R. A. *J. Phys. Chem. B* **1998**, *102*, 7910. (c) Ueno, A.; Suzuki, I.; Osa, T. *Anal. Chem.* **1990**, *62*, 2461.



^a Reagents and conditions: (i) ethylene glycol, pyridine, CH₂Cl₂, RT, 24 h; (ii) benzene, pyridine, ketene, reflux, 1 h; (iii) benzaldehyde, NH₄OAc, 100 °C, 30 min.

it seems advisable to restrict mutual approach of the two pyrene-based terminals. This goal could, in principle, be achieved by appending suitable blocking groups onto each pyrene unit or by using a central core that would hinder intramolecular association. The latter option was chosen for synthetic reasons because adding bulky groups to pyrene is a challenging operation.

Hantzsch DHP compounds⁴⁰ were identified as suitable candidates for the central core, because they are readily derivatized with aryl blocking groups and can be functionalized via the ester linkage. Moreover, such materials have found applications as effective calcium antagonists in that they inhibit the movement of calcium ions through certain membrane channels.⁴¹ It is interesting to note that their mode of action is associated with interactions at specific membrane sites. This additional biological role could offer the potential exploration of membrane properties and the measurement of ion transport phenomena using a DF probe.

Illustrated in Scheme 1 is the synthetic outline used for isolation of the prototype dyad PDHP. Reaction of pyrene-1-carbonyl chloride with an excess of ethylene glycol in the presence of base afforded the ester **1** in a nonoptimized 68% yield. This derivative was converted to **2** by reaction with diketene, again in high yield. Although there are a number of procedures for preparing DHP derivatives,⁴⁰ we found direct condensation in the absence of solvent to be the most appropriate methodology. Thus, heating **2** with benzaldehyde in the presence of ammonium acetate at 120 °C for 30 min afforded, after purification, PDHP. The low yield (6%) is typical for this type of reaction and represents the rigorous purification required to obtain samples suitable for the spectroscopic studies.

The electrochemical properties of PDHP were studied by cyclic voltammetry in dried CH₂Cl₂ containing *N*-tetrabutylammonium tetrafluoroborate (0.2 M) as background electrolyte and with ferrocene as the internal reference. On cathodic scans, the cyclic voltammograms showed only a solitary, quasi-reversible, two-electron wave ($\Delta E = 80$ mV)

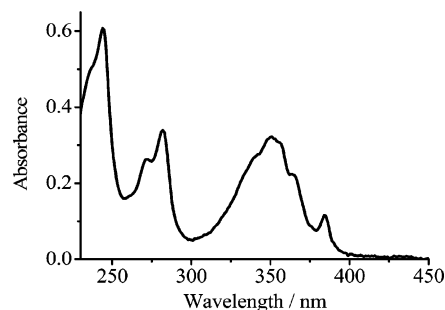


Figure 1. Absorption spectrum recorded for PDHP in cyclohexane solution.

centered at -1.65 V versus SCE. This wave can be assigned to the simultaneous one-electron reduction of each pyrene unit. There are no indications for communication between the two pyrene groups under these conditions. On oxidative sweeping, two irreversible waves are seen. The first step corresponds to a one-electron oxidative process, with the peak being centered at 1.18 V versus SCE. This wave is attributed to the one-electron oxidation of a pyrene unit, followed by fast association with a second pyrene so as to form the pyrene π -radical dimer.⁴² The second wave is due to a two-electron process and has the peak centered at 1.38 V vs SCE. This latter step is attributed to the two-electron oxidation of the central core. Indeed, oxidation of DHP derivatives is believed to involve loss of two electrons and a proton to give the corresponding *N*-pyridinium cation.⁴³ Interestingly, on the reverse scan sweep an irreversible cathodic wave was visible at approximately 0.76 V versus SCE, but only after oxidation, that might be attributable to the *N*-pyridinium salt.⁴⁴

Photophysical Properties. The absorption spectrum of PDHP recorded in cyclohexane solution shows a series of bands in the near-UV region (Figure 1). The lowest-energy transition appears at 382 nm as a shoulder on a more intense set of transitions centered at 348 nm ($\epsilon_{\text{MAX}} = 35\,350 \text{ M}^{-1} \text{ cm}^{-1}$). Additional sets of transitions are seen at around 280 nm ($\epsilon_{\text{MAX}} = 35\,200 \text{ M}^{-1} \text{ cm}^{-1}$) and at 240 nm ($\epsilon_{\text{MAX}} = 68\,100 \text{ M}^{-1} \text{ cm}^{-1}$). The lowest-energy absorption bands are assignable to the pyrene moieties and the overall absorption spectral profile resembles that expected for a pyrene carboxylate.⁴⁵ Weak transitions localized on the DHP unit are expected around 300 nm but are hidden beneath the more intense bands associated with the polycycle. The absorption spectrum is independent of concentration over a reasonable range and insensitive to changes in solvent polarity.

Fluorescence is readily observed in deoxygenated cyclohexane (Figure 2). Two regions of interest are apparent. A series of well-resolved transitions are seen across the range $380 < \lambda < 450$ nm that can be assigned to fluorescence from the monomer species by reference to the corresponding compound possessing only a single pyrene unit. In addition, there is a broad, featureless fluorescence band centered at about 495 nm that can be attributed to excimer emission.⁴⁶

(40) Torchy, S.; Cordonnier, G.; Barbry, D.; Vanden Eynde, J. J. *Molecules* **2002**, *7*, 528.

(41) (a) Fosshem, R.; Svarteng, K.; Mostad, A.; Rømming, C.; Shefter, E.; Triggle, D. J. *J. Med. Chem.* **1982**, *25*, 126. (b) Joslyn, A. F.; Luchowski, E.; Triggle, D. J. *J. Med. Chem.* **1988**, *31*, 1489.

(42) Sessler, J. L.; Kubo, Y.; Harriman, A. *J. Phys. Org. Chem.* **1992**, *5*, 644.

(43) López-Alarcón, C.; Núñez-Vergara, J. J.; Sequella, J. A. *Electrochim. Acta* **2003**, *48*, 2505.

(44) Zhu, X. Q.; Li, H. R.; Li, Q.; Ai, T.; Lu, Y. T.; Yang, Y.; Cheng, J. P. *Chem.—Eur. J.* **2003**, *9*, 871.

(45) Hrdlovic, P.; Chmela, S. *J. Photochem. Photobiol., A.* **1998**, *118*, 137.

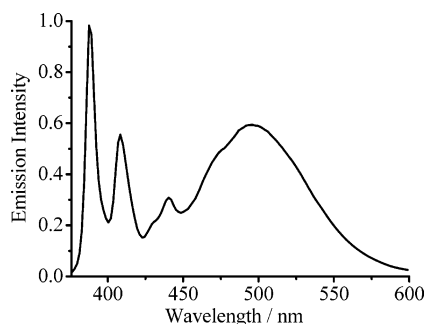


Figure 2. Fluorescence spectrum recorded for PDHP in deoxygenated cyclohexane at room temperature.

Table 1. Parameters Extracted from the Time-Resolved Fluorescence Decay Curves Collected for Monomer and Excimer Fluorescence from PDHP in Deoxygenated Cyclohexane at Room Temperature

parameter	monomer	excimer
A_1 , %	36	−37
τ_1 , ps	750	810
A_2 , %	62	−63
τ_2 , ns	4.7	4.4
A_3 , %	2	100
τ_3 , ns	25.9	26.3

The ratio of monomer to excimer fluorescence, measured by integration of the respective areas, is 0.40 ± 0.02 and remains independent of concentration over a 10^4 -fold dilution. This is clear indication that excimer formation occurs as a result of intramolecular interactions. The spectral pattern remains closely comparable in more polar solvents, although the ratio increases slightly with increasing dielectric constant of the solvent. Emission from the excimer is quenched on aeration of the solution, but the intensity of the monomer fluorescence is hardly affected by the presence of dissolved oxygen. In a glassy matrix at 77 K, formed with methylcyclohexane, only monomer fluorescence is observed. In fluid solution, the corrected fluorescence excitation spectrum was found to match well with the absorption spectrum recorded over the range $260 < \lambda < 400$ nm.

In deoxygenated cyclohexane at room temperature, the total fluorescence quantum yield (Φ_F) is 0.49 ± 0.02 . This can be compared to a value for the corresponding monomeric reference compound of $\Phi_F = 0.67 \pm 0.04$, where only monomer fluorescence is observed. Time-resolved fluorescence spectroscopy showed that the decay profiles recorded for monomer emission required analysis as the sum of three exponential components (Figure 3).⁴⁷ Thus, the fluorescence intensity (I_F) at time t could be well explained in terms of eq 1, where τ refers to a particular decay time and A is its fractional contribution to the total fluorescence signal at that wavelength. The derived decay times and fractional amplitudes are collected in Table 1. The same parameters were derived at different wavelengths across the range where the monomer emits. Complex decay kinetics were also recorded for excimer emission (Figure 4), and again it was necessary to consider the overall records in terms of three exponential components (Table 1). Here, excimer emission grows in after the excitation pulse, represented by the negative amplitudes given in Table 1, and decays on a much slower time scale.

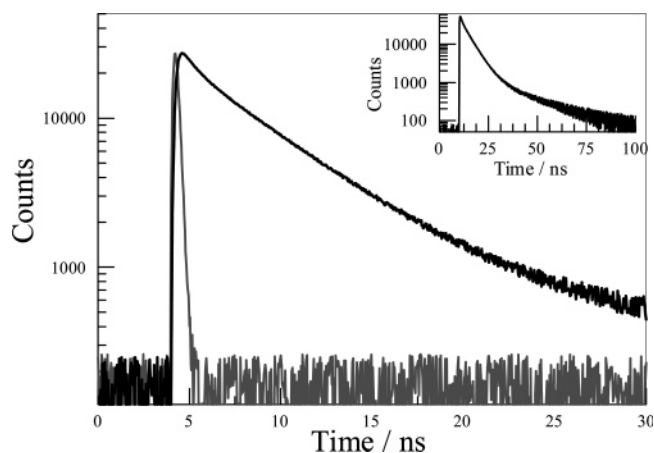


Figure 3. Fluorescence decay profile recorded for monomer emission at 395 nm from PDHP in deoxygenated cyclohexane at 20 °C. The inset shows a decay trace recorded on a longer time scale.

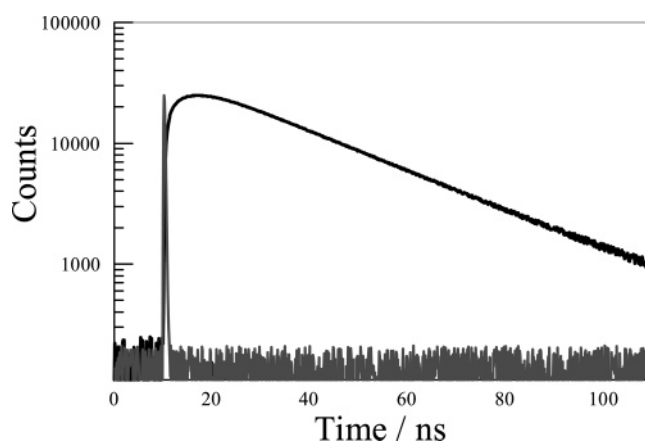


Figure 4. Fluorescence decay profile recorded for excimer fluorescence at 520 nm from PDHP in deoxygenated cyclohexane at room temperature.

Under the same conditions, fluorescence from the monomeric reference compound decays via first-order kinetics with a decay time of 12.6 ± 0.9 ns.

$$I_F(t) = A_1 e^{-t/\tau_1} + A_2 e^{-t/\tau_2} + A_3 e^{-t/\tau_3} \quad (1)$$

Fitting the time-resolved fluorescence data to eq 1 is clearly an approximation, and several other mathematical models could be used,⁴⁸ most notably τ_1 and τ_2 could be incorporated into a stretched exponential form.⁴⁹ The important point, however, is that the ground-state molecule appears to exist in families of conformations that differ in respect to the proximity of the two pyrene-based terminals. The shortest decay time, τ_1 , is attributed to folding within a closely spaced conformation. Attainment of the geometry necessary for excimer fluorescence is fast within this structure. A more extended conformation, where internal folding is slower, gives rise to the longer decay time, τ_2 . This latter decay time is not too far removed from that of the monomeric reference compound ($\tau = 12.6$ ns), thereby indicating that excimer formation is inefficient for this conformation. That excimer fluorescence grows in after the

(46) Birks, J. B. *Photophysics of Aromatic Molecules*; Wiley-Interscience: London, 1970.

(47) (a) Zachariasse, K. A.; Duveneck, G.; Busse, R. *J. Am. Chem. Soc.* **1984**, *106*, 1045. (b) Naumann, W. *J. Chem. Phys.* **2004**, *120*, 9618.

(48) Eaton, D. F. *Pure Appl. Chem.* **1990**, *62*, 1631.

(49) Włodarczyk, J.; Kierdaszuk, B. *Biophys. J.* **2003**, *85*, 589.

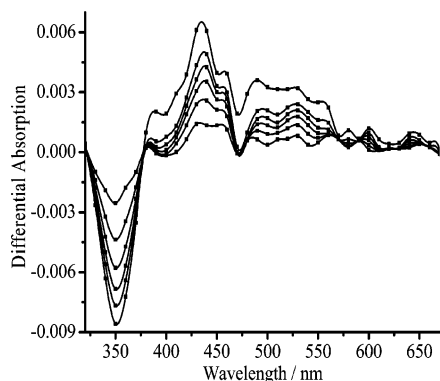


Figure 5. Triplet-triplet absorption spectra recorded after laser excitation of PDHP in deoxygenated cyclohexane at different delay times.

excitation pulse is clear evidence that the pyrene-based terminals are not stacked in the ground state and that folding is a necessary requisite for formation of the excimer. The combined decay records for monomer and excimer indicate that the longest decay time, τ_3 , is indicative of reversible dissociation of the excimer to reform the monomer. This component represents only a few percent of the total fluorescence attributable to the monomer, such that the principal routes for decay of the excimer involve steps other than dissociation to the monomer.

Excitation of PDHP in deoxygenated cyclohexane with a 4-ns laser pulse results in formation of the corresponding triplet excited state (Figure 5). The differential absorption spectrum recorded for the triplet state shows transient bleaching of the pyrene-based absorption bands located at around 350 nm together with absorption bands stretching between 400 and 600 nm. The signal decays via first-order kinetics with a decay time of $35 \pm 5 \mu\text{s}$ at low laser intensities. Increasing the laser intensity introduces a bimolecular component into the decay records because of TTA.⁵⁰ The triplet state is quenched by molecular oxygen. No other transient species are apparent in the spectral records and, in particular, there is no evidence to suggest that light-induced electron transfer occurs under these conditions.

Biphotonic Processes. At modest laser intensities, the decay profile recorded for the triplet state of PDHP in deoxygenated cyclohexane becomes non-exponential, and DF can be detected.⁵⁰ Both the total yield and the decay kinetics for this crop of DF depend on the initial concentration of the triplet state, the latter being varied by changes in either laser power or chromophore concentration. The spectral pattern recorded for the DF, taking due allowance of the greatly reduced precision inherent to laser flash photolysis relative to steady-state fluorescence spectroscopy, closely resembles that of the excimer (Figure 6). There is little, if any, contamination from fluorescence due to the monomer. This latter finding is entirely consistent with the realization that the excimer is formed quickly and is resistant to reversible dissociation to reform the excited-state monomer. Similar results were found in dichloromethane and propylene carbonate.

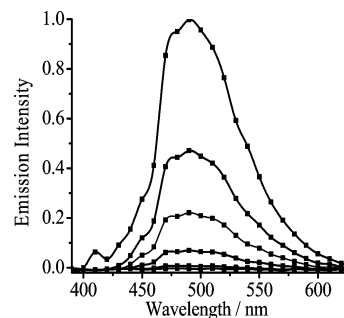


Figure 6. Spectral profile recorded for DF from PDHP in deoxygenated cyclohexane after exposure to saturating laser pulses (fwhm = 4 ns) delivered at 355 nm.

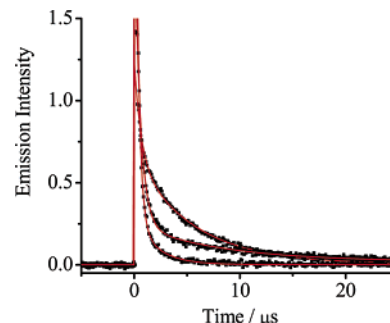


Figure 7. Examples of decay profiles recorded for DF from PDHP in deoxygenated cyclohexane. The three traces refer to different initial concentrations of PDHP, and the solid lines drawn through the data points refer to computer generated best fits to eq 2.

The DF decay profile recorded after irradiation of PDHP in deoxygenated cyclohexane with intense laser pulses shows two distinct temporal windows (Figure 7). The majority of the signal decays via first-order kinetics with an averaged decay time of $75 \pm 9 \text{ ns}$ that remains independent of the initial concentration of triplet state. This crop of DF arises from intramolecular TTA. On longer time scales, a second crop of DF is evident. This latter signal decays via mixed first- and second-order kinetics with a half-life that increases with decreasing initial concentration of the precursor triplet state. This event can be attributed to bimolecular contact between two PDHP molecules, each bearing a solitary triplet species. In this latter case, the decay time for DF corresponds to the decay time of the triplet precursors and is set by the rates of diffusional contact and inherent nonradiative decay.⁵¹ The relative ratio of the two crops of DF depends on the initial triplet concentration.

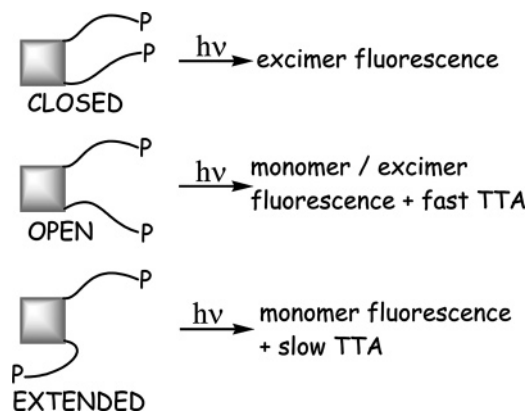
The overall decay kinetics for DF recorded after exposure to a saturating flash are well described in terms of eq 2,⁵² where the first term accounts for intramolecular TTA and the second term describes the corresponding bimolecular TTA step. Here, G_1 and G_2 , respectively, refer to the relative crops of intra- and intermolecular DF while k_{TT} is the rate constant for intramolecular TTA. The rate constant for bimolecular TTA is represented as k_{TTA} , and the initial concentration of the precursor triplet state is designated as $[T^*]$. The remaining parameter, k_{D} , refers to the inherent rate constant for nonradiative decay of the triplet state in the

(50) (a) Minaev, B. F. *Russ. Phys. J.* **1978**, *21*, 1120. (b) Tanaka, I.; Tokito, S. *J. Appl. Phys.* **2005**, *97*, 113531. (c) Rothe, C.; Al Attar, H. A.; Monkman, A. P. *Phys. Rev. B* **2005**, *72*, 155330. (d) Sapunov, V. V. *J. Appl. Spectrosc.* **2002**, *69*, 831.

(51) (a) Parker, C. A.; Joyce, T. A. *Chem. Commun.* **1967**, 744. (b) Krishna, V. G. *Chem. Phys.* **1967**, *46*, 1735. (c) Naqvi, K. R. *Chem. Phys. Lett.* **1968**, *1*, 561.

(52) Gehlen, M. H. *J. Phys. Chem.* **1995**, *99*, 4181.

Scheme 2. Cartoon Illustration of the Families of Conformations Proposed for PDHP and the Subsequent Fate of the Excited Singlet State^a



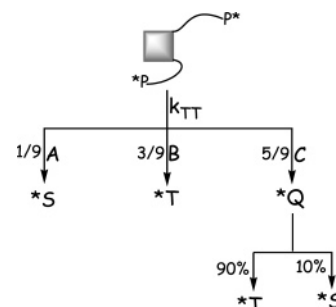
^a Note, intersystem crossing to the triplet manifold will accompany monomer fluorescence.

absence of TTA. This latter term ($k_D = 2.9 \times 10^4 \text{ s}^{-1}$) is known from the studies made at very low laser intensities. Evaluation of this equation across a range of laser intensities and initial concentrations allows computation of k_{TT} as being $1.3 \pm 0.2 \times 10^7 \text{ s}^{-1}$ and k_{TTA} as being $9 \pm 3 \times 10^8 \text{ M}^{-1} \text{ s}^{-1}$ at room temperature. The latter rate constant is somewhat less than the diffusion-controlled rate limit ($k_{\text{DIFF}} = 6 \times 10^9 \text{ M}^{-1} \text{ s}^{-1}$) under these conditions, showing the difficulties associated with obtaining an appropriate structural arrangement for energy transfer. Indeed, triplet-energy transfer demands orbital contact between the reacting pyrene triplets, and this is rendered difficult by the large size and high flexibility of PDHP in solution. Bimolecular TTA is well-known in pyrene derivatives,⁵³ but the intramolecular equivalent has received little investigation.⁵⁴

$$I_{\text{DF}}(t) = G_1 e^{-k_{TT}t} + G_2 \left\{ \frac{e^{-k_D t}}{[T^*]^{-1} + (1 - e^{-k_D t})(2k_{TTA}/k_D)} \right\}^2 \quad (2)$$

The most interesting feature of this analysis, at least in terms of molecular imaging, concerns the intramolecular TTA process. This step dominates under conditions of high laser intensities and at intermediate concentrations of chromophore. The time scale for intramolecular DF, as expressed in terms of the inverse rate constant, is approximately 75 ns and is much longer than the time taken to form the excimer from the first excited singlet state. Indeed, two families of molecular conformations have been shown to fold into the required excimer geometry with approximate time constants of 0.8 and 5 ns, respectively (Scheme 2). It is presumed that these conformations differ by virtue of the initial proximity of the pyrene-based terminals. To account for the observed DF kinetics it is necessary to propose that there exists a third group of molecular conformations that does not undergo

Scheme 3. Outline of the Processes that Follow from Biphotonic Excitation of the Extended Conformation Proposed for PDHP^a



^a See the text for further details.

excimer formation on the available time scale (Scheme 2). Light absorption within this particular conformation promotes both pyrene terminals to the first excited singlet state and is followed by intersystem crossing to the triplet manifold. Internal folding is relatively slow for this extended conformation and is characterized by the 75 ns decay time.⁵⁵

Intramolecular TTA is a rather complicated process and can be considered in terms of Scheme 3. Thus, based on the mechanism evaluated for the corresponding bimolecular step,⁵⁶ intramolecular TTA can be partitioned between three competing routes that are subject to spin restriction rules.⁵⁷ Route A, which occurs at one-ninth the diffusion-controlled rate limit, leads to formation of the first excited singlet state localized on one of the pyrene moieties and is responsible for the major yield of DF. Route B involves dissociation of the triplet encounter complex in favor of the triplet state. Route C forms a quintet encounter complex⁵⁸ that itself partitions to give a minor crop of DF and the triplet state. This competition serves to minimize the quantum yield for DF and to lower the decay time of the triplet state. As a consequence, DF appears in quite low yield but with a modest prolongation of the decay time relative to the corresponding monophotonic process. In the case of PDHP in cyclohexane, this extension of the decay time amounts to a factor of approximately three-fold.

Concluding Remarks

Some attention has been given to the use of DF as an analytical tool, most notably in the form of an in situ temperature sensor,⁵⁹ while two-photon absorption techniques are becoming increasingly more popular due to the ready availability of high power lasers.⁶⁰ Rapid progress has also been made with regards to the development of phase-locked optical microscopes,⁶¹ where laser excitation can also result in high photon densities. Thermally activated DF is now an

- (53) (a) Birks, J. B. *Phys. Lett. A* **1967**, 24A, 479. (b) Birks, J. B.; Srinivasan, B. N.; McGlynn, S. P. *J. Mol. Spectrosc.* **1968**, 27, 266.
 (54) (a) Cai, J. J.; Lim, E. C. *J. Phys. Chem.* **1994**, 98, 2515. (b) Stelmakh, G. F.; Tsvirko, M. P. *Khim. Fiz.* **1986**, 5, 1322. (c) Helene, C.; Longworth, J. W. *J. Chem. Phys.* **1972**, 57, 399. (d) Monkman, A. P.; Burrows, H. D.; Hamblett, I.; Navaratnam, S. *Chem. Phys. Lett.* **2001**, 340, 467.

- (55) Rettig, W.; Paeplow, B.; Herbst, H.; Mullen, K.; Desvergne, J. P.; Bouas-Laurent, H. *New J. Chem.* **1999**, 23, 453.
 (56) Charlton, J. L.; Dabestani, R.; Saltiel, J. *J. Am. Chem. Soc.* **1983**, 105, 3473.
 (57) Saltiel, J.; Marchand, G. R.; Smothers, W. K.; Stout, S. A.; Charlton, J. L. *J. Am. Chem. Soc.* **1981**, 103, 7159.
 (58) Porter, G.; Wright, M. R. *Discuss. Faraday Soc.* **1959**, 27, 18.
 (59) Baleizao, C.; Berberan-Santos, M. N. *J. Fluoresc.* **2006**, 16, 215.
 (60) Service, R. F. *Science* **2003**, 301, 154.
 (61) Atia, W. A.; Davis, C. C. *Appl. Phys. Lett.* **1997**, 70, 405.

accepted form of molecular imaging⁶² where the improved temporal resolution discriminates against light scattering, reflection, autofluorescence, and extraneous prompt fluorescence. The result is vastly improved contrast, especially in cases where the ratio of delayed to prompt fluorescence can be used as the diagnostic parameter. Until now, little if any attention has been given to the development of imaging reagents capable of biphotonic DF of the type described above. There is, however, considerable interest in such events taking place in conducting polymers because these represent energy wastage.⁶³

The main advantage of biphotonic DF is that the approach favors formation of the excimer. This helps to prolong the decay time of the emitting species and expand the Stokes' shift. Only the intramolecular case need be considered, but this necessitates the use of relatively large molecules that might be difficult to accommodate in the host medium. A further problem concerns the need to exclude molecular oxygen, but this is common to all imaging systems based on long-lived emission. The quantum yield for DF from PDHP in deoxygenated cyclohexane is estimated to be around 2% by reference to phosphorescence from ruthenium-(II) tris(2,2'-bipyridine). This low yield reflects, in part, the spin restriction rules⁵⁷ that control formation of the excited singlet state during TTA and also the inherent quantum yield for formation of the triplet state. This latter parameter can be increased dramatically by the heavy-atom effect,⁶⁴ as illustrated in Figure 8 where the effect of added iodoethane

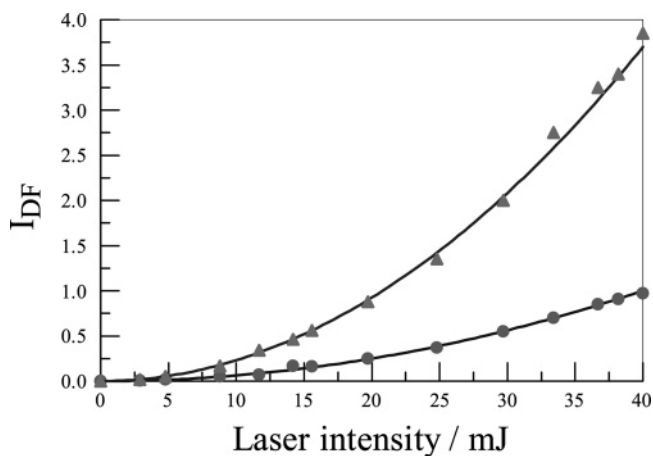


Figure 8. Effect of laser intensity on the yield of DF observed for PDHP in deoxygenated cyclohexane in the absence (●) and presence (▲) of iodoethane (10% v/v).

is considered. The fact that the DF signal depends on the square of the incident laser intensity (Figure 8) aids the separation of the required signal from background artifacts. Finally, the actual DF decay time is set by local phenomena such as the molecular conformation and the microviscosity of the surrounding medium, and these might be exploited to good effect. Further studies are in progress with a view to developing next-generation prototypes capable of improved optical properties.

Acknowledgment. We thank EPSRC (EP/D001994/1) and Newcastle University for financial support.

CM062525H

- (62) (a) Johnson, P.; Garland, P. B. *Biochem. J.* **1982**, 203, 313. (b) Pravinata, L. C.; You, Y.; Ludescher, R. D. *Biophys. J.* **2005**, 88, 3551.
- (63) (a) Partee, J.; Frankevich, E. L.; Uhlhorn, B.; Shinar, J.; Ding, Y.; Barton, T. J. *Phys. Rev. Lett.* **1999**, 82, 3673. (b) Bodunov, E. N.; Berberan-Santos, M. N.; Martinho, J. M. G. *Chem. Phys.* **2005**, 316, 217. (c) Barzykin, A. V.; Tachiya, M. *J. Phys. Chem. B* **2006**, 110, 7068.

- (64) McGlynn, S. P.; Azumi, T.; Kinoshita, M. *Molecular Spectroscopy of the Triplet State*; Prentice Hall: Englewood Cliffs, NJ, 1969.